Inorganic Chemistry

Article

pubs.acs.org/IC

Anion and Solvent Induced Chirality Inversion in Macrocyclic Lanthanide Complexes

Aleksandra Gerus, Katarzyna Ślepokura, and Jerzy Lisowski*

Department of Chemistry, University of Wrocław, 14 F. Joliot-Curie, 50-383 Wrocław, Poland

Supporting Information

ABSTRACT: A series of the lanthanide(III) or yttrium(III) complexes of the type $[LnL(NO_3)(H_2O)_2](NO_3)_2$, $[LnL(NO_3)(H_2O)](NO_3)_2$, $[LnL(H_2O)_2](NO_3)_3$, and $[LnLCl(H_2O)_2]Cl_2$ where L is an all-*R* or all-*S* enantiomer (L^R or L^S) of the chiral hexaaza macrocycle, 2(*R*),7(*R*),18(*R*),23(*R*)- or 2(*S*),7(*S*),18(*S*),23(*S*)-1,8,15,17,24,31-hexaazatricyclo[25.3.1.1.0.0]-dotriaconta-10,12,14,26,28,30-hexaene, and Ln(III) = Sm(III), Tb(III), Ho(III), Er(III), Tm(III), Yb(III), Lu(III), or Y(III), have been synthesized and structurally characterized. The crystal structure of the free macrocycle shows a highly twisted molecule, preorganized for the formation of helical complexes. The crystal structures of the lanthanide(III) complexes show two different diastereomeric forms of the macrocycle with different configurations at the stereogenic amine nitrogen atoms: (*RRRR*) or (*RSRS*) (denoted as L^{RI} and L^{RII}, respectively). The L^{RI} diastereomeric form of the nitrate derivatives $[LnL(NO_3)(H_2O)](NO_3)_2$ (Ln = Ho, Er) and $[LnL(H_2O)_2](NO_3)_3$ (Ln = Tm, Yb, Lu) convert slowly to the L^{RII} form in methanol or acetonitrile solutions, while this process is not observed for the L^{RI} diastereomers of analogous chloride derivatives $[LnL(H_2O)_2]Cl_3$ (Ln = Tm, Yb, Lu). On the other hand, the $L^{RI} \rightarrow L^{RII}$ conversion for these Tm(III), Yb(III), and Lu(III) chloride derivatives can be triggered by the addition of external nitrate anions. The circular dichroism (CD) and ^{1}H NMR data indicate initial fast exchange of axial chloride for axial nitrate ligand, followed by slow chirality inversion of the equatorial macrocyclic ligand.

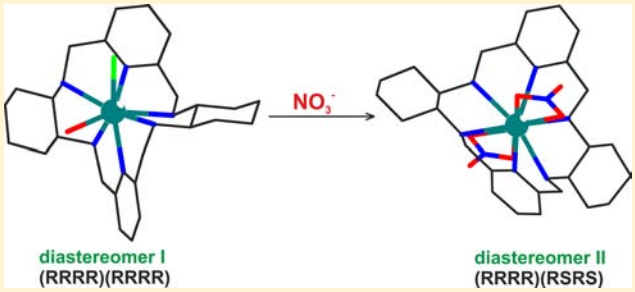

INTRODUCTION

Macrocyclic lanthanide(III) and chiral lanthanide(III) complexes attract considerable attention because of their unique properties and potential applications. Robust Ln(III) complexes of defined chirality may be effectively obtained by the application of enantiopure macrocyclic ligands. For instance, the enantiopure macrocyclic complexes derived from 2,6-pyridinedicarboxaldehyde and *trans*-(1*R*,2*R*)-diaminecyclohexane form a number of metal complexes,[1−6] which have been studied in the context of helicity inversion,[1,5] chiral self-recognition,[3a] axial ligand exchange,[3b] chirooptical properties,[3e,5a] interactions with DNA[4] and formation of polymetallic systems.[3a,6] In particular the 2 + 2 chiral hexaaza tetraamine macrocycle L (Figure 1) derived from the above precursors forms both enantiopure[1] and racemic[2] lanthanide(III) complexes. The chirality of free L is determined by the configuration at the stereogenic cyclohexane carbon atoms, and this macrocycle can be easily obtained in enantiopure form as either all-*R* or all-*S* enantiomer (denoted as L^R and L^S). In the rigid complexed form of this macrocyle the configuration at the amine nitrogen atoms is fixed, that in principle creates new stereogenic centers and new isomeric forms. This type of isomerism plays an important role in the chemistry of complexes of tetraazamacrocyclic amines, where different diastereomeric forms are determined by the configuration at nitrogen atoms.[7,8] We have previously shown that this type of isomerism plays a role also in the chemistry of hexaazamacrocycles and that the lanthanide(III) complexes of L^R can exist in two diastereomeric forms, which differ in the sense of helical twist and the configuration at the stereogenic amine nitrogen atoms.[1] In one of the stereoisomers, denoted as L^{RI}, the macrocycle L^R of (*RRRR*) configuration at the stereogenic cyclohexane carbon atoms adopts (*RRRR*) configuration at the amine nitrogen atoms, while in the other stereoisomer, denoted as L^{RII}, the macrocycle L^R adopts (*RSRS*) configuration at the amine nitrogen atoms (Figure 1). In the case of the nitrate Yb(III) complex it was shown that the L^{RI} and L^{RII} diastereomers can be selectively interconverted by changing the solvent (water vs acetonitrile), which represents a rare case of helicity inversion controlled by the solvent. In this contribution we extend this process to the Ho(III), Er(III), Tm(III), and Lu(III) complexes. We also show that this interconversion is anion dependent; while it is operating in the case of the nitrate derivatives, it is not observed for the analogous chloride derivatives of the type $[LnL^{RI}(H_2O)_2]Cl_3$. For the latter complexes, however, the chirality inversion can be triggered in organic solvents by the replacement of the axial Cl^- anion for the NO_3^- anion.

Controlled chirality switching is a rare process occurring in various systems such as metal complexes, DNA, supramolecular

Received: June 6, 2013
Published: October 22, 2013

   dx.doi.org/10.1021/ic401437r | *Inorg. Chem.* 2013, 52, 12450−12460

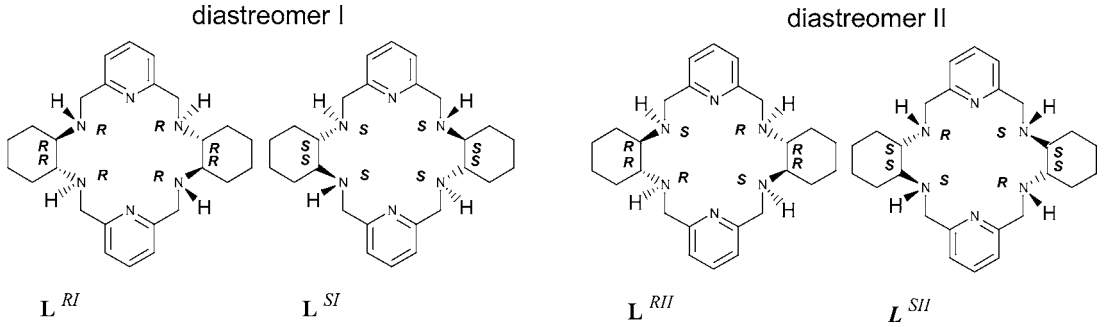

Figure 1. Stereomers of the chiral macrocycle L.

assemblies, and as organic polymers.[9−12] Inversion of helical conformation may correspond to the conversion of kinetic product to the thermodynamic product or can be triggered by stimuli such as change of solvent, redox process, or light. In particular, the Miyake group has demonstrated the selective switching of helicity of a chiral tetradentate ligand triggered by the exchange of achiral anion in the metal coordination sphere.[10f,g,k,l] Helicity inversion triggered by achiral anions has also been observed for organic foldamers.[12]

EXPERIMENTAL SECTION

Measurements. The NMR spectra were taken on Bruker Avance 500 and AMX 300 spectrometers. The pH* readings for the D_2O solutions were converted to pH values as described previously.[13] The circular dichroism (CD) spectra were measured on Jasco J-715 Spectropolarimeter. The electrospray mass were obtained using a Bruker microOTOF-Q instrument. The elemental analyses were carried out on a Perkin-Elmer 2400 CHN elemental analyzer.

Crystal Structure Determination. The crystals of free ligand trichloromethane disolvate ($L^R{\cdot}2CHCl_3$) suitable for single-crystal X-ray diffraction experiments were grown from chloroform. The crystals of $[HoL^{RI}(NO_3)(H_2O)](NO_3)_2{\cdot}0.4H_2O$, $[ErL^{RI}(NO_3)(H_2O)](NO_3)_2{\cdot}0.3H_2O$, $[TmL^{RI}(H_2O)_2](NO_3)_3{\cdot}H_2O$ and $[LuL^{RI}(H_2O)_2](NO_3)_3{\cdot}H_2O$ were obtained by slow evaporation of the water solutions of the $[HoL^{RI}(NO_3)(H_2O)](NO_3)_2$, $[ErL^{RI}(NO_3)(H_2O)](NO_3)_2$, $[TmL^{RI}(H_2O)_2](NO_3)_3$, and $[LuL^{RI}(H_2O)_2](NO_3)_3$ complexes, respectively. The crystals of $[YbL^{RI}Cl(H_2O)]Cl_2{\cdot}CH_3CN$ and $[YL^{RI}Cl(H_2O)]Cl_2{\cdot}MeOH{\cdot}2H_2O$ have been obtained from the acetonitrile solution of $[YbL^{RI}(H_2O)_2]Cl_3$ and from the methanol solution of $[YL^{RI}(H_2O)_2]Cl_3$, respectively. The crystals of $[SmL^{RII}(NO_3)(H_2O)_2](NO_3)_2$ and $[TbL^{RII}(NO_3)(H_2O)](NO_3)_2{\cdot}0.3H_2O$ were grown by slow evaporation of the methanol/acetonitrile 1:1 solutions of $[SmL^{R}(NO_3)(H_2O)_2](NO_3)_2$ and $[TbL^{R}(NO_3)(H_2O)](NO_3)_2$ complexes, respectively.

The crystallographic measurements were performed at 100−296(2) K (Table 1) on a κ-geometry Xcalibur PX (ω and φ scan), Xcalibur R (ω scan) or Kuma KM4CCD (ω scan) four-circle diffractometers with graphite-monochromatized MoK_α radiation. Data were corrected for Lorentz and polarization effects. Data collection, cell refinement, data reduction, and analysis were carried out with Crysalis CCD and Crysalis RED, respectively.[14] Analytical or empirical (multiscan) absorption correction was applied to the data with the use of Crysalis RED. The structures of free ligand chloroform disolvate ($L^R{\cdot}2CHCl_3$) and the complexes $[HoL^{RI}(NO_3)(H_2O)](NO_3)_2{\cdot}0.4H_2O$, $[YL^{RI}Cl(H_2O)]Cl_2{\cdot}MeOH{\cdot}2H_2O$, $[YbL^{RI}Cl(H_2O)]Cl_2{\cdot}CH_3CN$, and $[TbL^{RII}(NO_3)(H_2O)](NO_3)_2{\cdot}0.3H_2O$ were solved by direct methods using the SHELXS-97 program[15] and refined on F^2 by a full-matrix least-squares technique using SHELXL-2013[15] with anisotropic thermal parameters for the ordered and fully occupied non-H atoms. Some of the not fully occupied positions were also refined anisotropically. Because the erbium complex $[ErL^{RI}(NO_3)(H_2O)](NO_3)_2{\cdot}0.3H_2O$ is isomorphous with $[HoL^{RI}(NO_3)(H_2O)](NO_3)_2{\cdot}0.4H_2O$, the refinement of its structure was started by using the coordinates of ordered heavy atoms taken from the holmium complex. A similar procedure was applied to the $[TmL^{RI}(H_2O)_2](NO_3)_3{\cdot}H_2O$ and $[LuL^{RI}(H_2O)_2](NO_3)_3{\cdot}H_2O$ complexes, which were refined using starting coordinates taken from the isomorphous ytterbium complex reported previously,[1] and to $[SmL^{RII}(NO_3)(H_2O)_2](NO_3)_2$, which was based on *x*, *y*, *z* from the isomorphous europium complex.[1] Figures presenting the molecular structures were made using the Diamond[16] program. The details of structure refinement and the description of disorder are provided in the Supporting Information.

Syntheses. Macrocycle L^R and the $[YbL^{RI}(H_2O)_2](NO_3)_3$ complex were obtained as previously described.[1] The enantiomers L^S and $[YbL^{SI}(H_2O)_2](NO_3)_3$ were obtained in a similar fashion.

$[HoL^{RI}(NO_3)(H_2O)](NO_3)_2$. A 88.2 mg portion (0.2 mmol) of $Ho(NO_3)_3{\cdot}5H_2O$ and 86.9 mg (0.2 mmol) of macrocycle L^R were dissolved in 3 mL of water, and the mixture was refluxed for 2 h. The obtained clear solution was cooled down and left to concentrate slowly in air (to ca. 1 mL). The obtained crystalline white product was filtered and dried in vacuum. Yield 93 mg (56%). ^{1}H NMR (300 MHz, D_2O, 298 K): −136.59, −76.71, −27.48, 10.64, 20.95, 41.02, 57.84, 70.55, 80.81, 103.78, 145.62 ppm. Calcd (anal.) for $HoC_{26}H_{46}N_9O_{13}$: C, 35.98 (36.41); H, 4.55 (5.41); N, 14.77 (14.70).

The $\mathbf{[ErL^{RI}(NO_3)(H_2O)](NO_3)_2}$, $\mathbf{[TmL^{RI}(H_2O)_2](NO_3)_3}$, $\mathbf{[LuL^{RI}(H_2O)_2](NO_3)_3}$ complexes were obtained in a similar fashion.

$[ErL^{RI}(NO_3)(H_2O)](NO_3)_2$. Yield 92 mg (56%). ^{1}H NMR (300 MHz, D_2O, 298 K): −123.71, −100.20, −70.82, −39,23, −18.37, −7.57, 10.58, 19.37, 29.38, 42.75, 204.08. Calcd (anal.) for $ErC_{26}H_{46}N_9O_{13}$: C, 36.13 (36.31); H, 5.34 (5.39); N, 14.69 (14.66).

$[TmL^{RI}(H_2O)_2](NO_3)_3$. Yield 98 mg (57%). ^{1}H NMR (300 MHz, D_2O, 298 K): −272.00, −211.16, −181.52, −172.37, −81.22, −53.82, −32.54, −13.67, −12.02, 7.94, 28.45, 31.00, 38.98, 69.59, 96.25, 107.53. Calcd (anal.) for $TmC_{26}H_{46}N_9O_{13}$: C, 35.75 (36.24); H, 4.93 (5.38); N, 14.59 (14.63).

$[LuL^{RI}(H_2O)_2](NO_3)_3$. Yield 102 mg (61%). ^{1}H NMR (500 MHz, D_2O, 298 K): 0.94, 1.21, 1.33, 1.84, 2.28, 2.43, 2.52, 2.71, 3.56, 4.17, 4.39, 4.42, 4.60, 4.63, 4.66, 7.59, 8.11. Calcd (anal.) for $LuC_{26}H_{46}N_9O_{13}$: C, 36.15 (35.99); H, 5.10 (5.43); N, 14.61 (14.53).

The $[SmL^{R}(NO_3)(H_2O)_2](NO_3)_2$ and $[TbL^{R}(NO_3)(H_2O)](NO_3)_2$ complexes were obtained in a similar fashion as the above complexes, but they were further recrystallized from chloroform−methanol (1:1) solutions.

$[SmL^{RII}(NO_3)(H_2O)_2](NO_3)_2$. Yield 87 mg (54%). ^{1}H NMR (500 MHz, $CDCl_3/CD_3OH$ v/v 1/1, 298 K): 1.70, 2.12, 2.29, 2.60, 2.71, 3.45, 4.17, 4.29, 5.10, 5.22, 5.42, 5.92, 6.13, 7.27, 7.70, 7.85, 11.48. Calcd (anal.) for $SmC_{26}H_{42}N_9O_{11}$: C, 38.32 (38.69); H, 5.16 (5.25); N, 15.47 (15.62).

$[TbL^{RII}(NO_3)(H_2O)](NO_3)_2$. Yield 87 mg (53%). ^{1}H NMR (500 MHz, $CDCl_3/CD_3OH$ v/v 1/1, 298 K): −16.30, −7.34, −5.94, 1.63, 21.91, 22.88, 26.22, 26.75, 38.84, 52.40, 55.16, 58.71, 93.92, 105.19, 112.44, 136.77, 222.39.

$[LnL^{RI}(H_2O)_2]Cl_3$ complexes. A 0.5 mmol portion of appropriate lanthanide(III) or yttrium(III) chloride hydrate and 217.3 mg (0.5 mmol) of macrocycle $L^{(RRRR)}$ were dissolved in 5 mL of water, and the mixture was refluxed for 2 h. The obtained clear solution was cooled down and left to concentrate slowly in air (to ca. 1 mL). The obtained white product was filtered and dried in vacuum.

dx.doi.org/10.1021/ic401437r | Inorg. Chem. 2013, 52, 12450−12460

Table 1. Crystallographic Data of the Compounds

	$L{\cdot}2CHCl_3$	$[HoL(NO_3)(H_2O)]{\cdot}(NO_3)_2{\cdot}0.4H_2O$	$[ErL(NO_3)(H_2O)]{\cdot}(NO_3)_2{\cdot}0.3H_2O$	$[TmL(H_2O)_2]{\cdot}(NO_3)_3{\cdot}H_2O$	$[LuL(H_2O)_2]{\cdot}(NO_3)_3{\cdot}H_2O$	$[YLCl(H_2O)]Cl_2{\cdot}MeOH{\cdot}2H_2O$	$[YbLCl(H_2O)]Cl_2{\cdot}CH_3CN$	$[SmL(NO_3)(H_2O)_2]{\cdot}(NO_3)_2$	$[TbL(NO_3)(H_2O)]{\cdot}(NO_3)_2{\cdot}0.3H_2O$
empirical formula	$C_{28}H_{40}Cl_6N_6$	$C_{26}H_{40.8}HoN_9O_{10.4}$	$C_{26}H_{40.6}ErN_9O_{10.3}$	$C_{26}H_{44}N_9O_{12}Tm$	$C_{26}H_{44}LuN_9O_{12}$	$C_{27}H_{48}Cl_3N_6O_4Y$	$C_{28}H_{43}Cl_3N_7OYb$	$C_{26}H_{42}N_9O_{11}Sm$	$C_{26}H_{40.6}N_9O_{10.3}Tb$
fw (g mol^{-1})	673.36	810.80	811.33	843.63	849.67	715.97	773.08	807.03	802.99
cryst syst	monoclinic	orthorhombic	orthorhombic	orthorhombic	orthorhombic	orthorhombic	orthorhombic	monoclinic	monoclinic
space group	$C2$ (No. 5)	$P2_12_12_1$ (No.19)	$P2_12_12_1$ (No.19)	$P2_12_12_1$ (No.19)	$P2_12_12_1$ (No.19)	$P2_12_12_1$ (No.19)	$P2_12_12_1$ (No.19)	$P2_1$ (No. 4)	$C2$ (No. 5)
a (Å)	14.230(5)	10.696(3)	10.673(3)	10.692(3)	10.690(3)	8.138(2)	7.969(2)	14.358(5)	20.453(5)
b (Å)	10.235(3)	15.383(4)	15.323(6)	12.469(3)	12.451(3)	16.612(3)	18.679(5)	15.289(5)	15.180(3)
c (Å)	11.719(3)	18.385(7)	18.406(6)	24.045(6)	24.008(4)	23.266(5)	20.558(5)	15.568(4)	11.963(4)
β (deg)	96.81(3)							105.24(3)	117.12(3)
V (Å^3)	1694.8(9)	3025.0(16)	3010.2(18)	3205.6(14)	3195.5(13)	3145.3(12)	3060.1(13)	3297.3(18)	3305.9(17)
Z	2	4	4	4	4	4	4	4	4
T (K)	296(2)	100(2)	100(2)	100(2)	100(2)	100(2)	102(2)	296(2)	296(2)
D_{calcd} (g cm^{-3})	1.320	1.780	1.790	1.748	1.766	1.512	1.678	1.626	1.613
μ (mm^{-1})	0.54	2.69	2.86	2.84	3.17	2.15	3.35	1.85	2.21
cryst size (mm)	0.23 × 0.09 × 0.07	0.19 × 0.16 × 0.09	0.19 × 0.17 × 0.07	0.34 × 0.13 × 0.05	0.23 × 0.17 × 0.09	0.40 × 0.34 × 0.08	0.21 × 0.15 × 0.06	0.18 × 0.17 × 0.03	0.20 × 0.19 × 0.03
radiation type	Mo Kα	Mo Kα	Mo Kα	Mo Kα	Mo Kα	Mo Kα	Mo Kα	Mo Kα	Mo Kα
λ (Å)	0.71073	0.71073	0.71073	0.71073	0.71073	0.71073	0.71073	0.71073	0.71073
θ range (deg)	2.88−28.69	4.77−27.99	2.88−28.00	4.71−28.00	3.03−29.00	2.92−36.80	2.78−31.10	2.90−28.87	2.94−28.88
index ranges	$-17 \le h \le 17$	$-9 \le h \le 14$	$-14 \le h \le 11$	$-10 \le h \le 14$	$-14 \le h \le 11$	$-12 \le h \le 13$	$-10 \le h \le 8$	$-18 \le h \le 12$	$-22 \le h \le 27$
	$-13 \le k \le 13$	$-19 \le k \le 12$	$-20 \le k \le 20$	$-16 \le k \le 16$	$-16 \le k \le 16$	$-25 \le k \le 27$	$-25 \le k \le 25$	$-19 \le k \le 20$	$-20 \le k \le 19$
	$-15 \le l \le 13$	$-24 \le l \le 22$	$-24 \le l \le 23$	$-31 \le l \le 31$	$-32 \le l \le 32$	$-38 \le l \le 35$	$-29 \le l \le 26$	$-18 \le l \le 19$	$-16 \le l \le 12$
T_{min}/T_{max}	0.853/1.000	0.895/1.000	0.958/1.000	0.576/0.863	0.504/0.778	0.496/0.838	0.518/0.821	0.845/1.000	0.652/0.939
measured reflns	5402	12343	25622	32691	41899	56084	27981	15768	10232
independent reflns	3463	7079	7220	7702	8450	15163	8356	12476	6464
obsd reflns ($I > 2\sigma(I)$)	1905	6335	6462	7462	8164	11849	7777	11157	5908
Rint	0.020	0.028	0.044	0.027	0.032	0.042	0.037	0.020	0.019
data/restraints/params	3463/62/216	7079/21/416	7220/21/416	7702/9/433	8450/9/433	15163/11/365	8356/2/362	12476/43/838	6464/10/417
$R1$, $wR2$[a] ($F_o^2 > 2\sigma(F_o^2)$)	0.050, 0.086	0.028, 0.048	0.026, 0.049	0.016, 0.036	0.015, 0.036	0.031, 0.053	0.025, 0.056	0.039, 0.066	0.025, 0.044
$R1$, $wR2$ (all data)	0.109, 0.108	0.035, 0.050	0.032, 0.050	0.017, 0.036	0.016, 0.036	0.050, 0.055	0.028, 0.057	0.047, 0.070	0.030, 0.046
GOF = S	1.02	1.00	1.00	1.01	1.03	1.01	1.01	1.00	1.01
$\Delta\rho_{max}/\Delta\rho_{min}$ (e Å^{-3})	0.12/−0.14	1.20/−0.66	1.25/−0.47	0.74/−0.32	1.00/−0.27	0.67/−0.78	1.16/−0.59	0.82/−0.72	0.78/−0.51
Flack parameter	0.04(4)	−0.020(6)	−0.015(5)	−0.027(2)	−0.017(3)	−0.0225(12)	−0.021(3)	−0.023(9)	0.003(8)

[a] $R1 = \sum||F_c| - |F_o||/\sum|F_o|$; $wR2 = (\sum[w(F_o^2 - F_c^2)^2]/\sum[w(F_o^2)^2])^{1/2}$. Detailed values of the weighting scheme (w) in each system are given in the crystallographic information file (CIF) provided as Supporting Information.

dx.doi.org/10.1021/ic401437r | Inorg. Chem. 2013, 52, 12450−12460

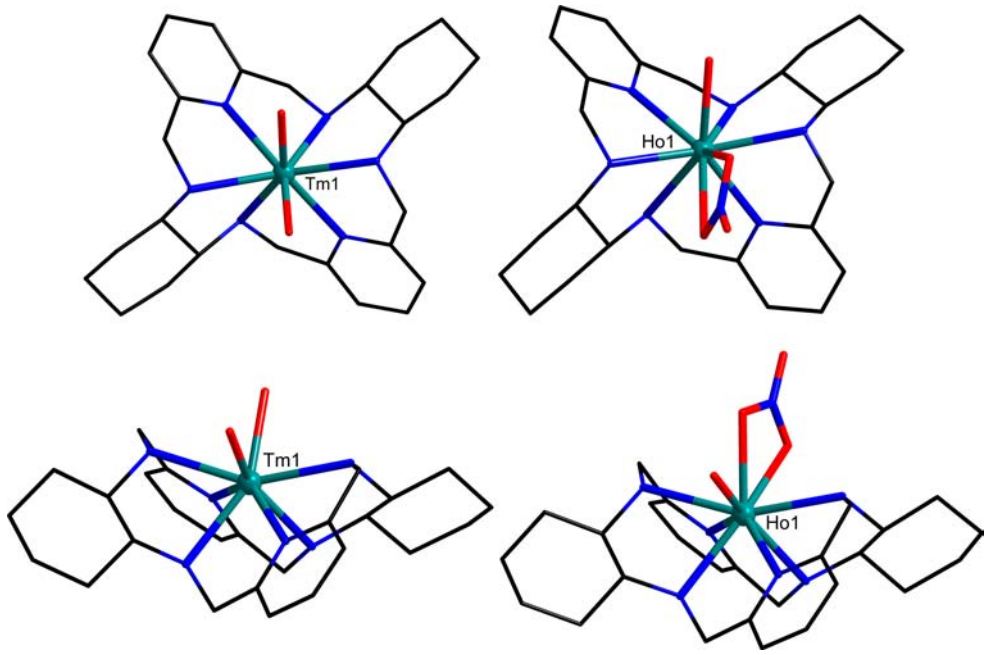

Figure 2. Structures of $[TmL^{RI}(H_2O)_2]^{3+}$ (left) and $[HoL^{RI}(NO_3)(H_2O)]^{2+}$ (right) complex cations.

$[TmL^{RI}(H_2O)_2]Cl_3$. Yield 228 mg (61%). ^{1}H NMR (300 MHz, D_2O, 298 K): −280.92, −217.08, −185.49, −176.41, −83.73, −54.70, −36.54, −14.31, −11.87, 8.59, 29.81, 31.33, 32.44, 38.83, 41.16, 72.41, 99.68, 110.22. Calcd (anal.) for $LuC_{26}H_{58}N_6O_{10}Cl_3$: C, 36.23 (36.57); H, 5.89 (5.80); N, 9.68 (9.84).

$[YbL^{RI}(H_2O)_2]Cl_3$. Yield 227 mg (61%). ^{1}H NMR (300 MHz, D_2O, 298 K): −75.91, 72.10, −70.02, −25.37, −22.03, −9.75, −2.13, −1.74, 1.03, 3.77, 5.80, 13.17, 16.98, 17.85, 24.75, 40.84, 48.85, 105.70. Calcd (anal.) for $YbC_{26}H_{54}N_6O_8Cl_3$: C, 36.11 (36.39); H, 5.23 (5.34); N, 9.57 (9.79).

$[LuL^{RI}(H_2O)_2]Cl_3$. Yield 232 mg (62%). ^{1}H NMR (500 MHz, D_2O, 298 K): 8.11, 7.59, 4.67, 4.64, 4.60, 4.42, 4.39, 4.18, 3.57, 2.71, 2.53, 2.43, 2.28, 1.84, 1.34, 1.21, 0.94. Calcd (anal.) for $LuC_{26}H_{60}N_6O_{11}Cl_3$: C, 35.73 (35.56); H, 5.18 (5.43); N, 9.44 (957).

$[YL^{RI}(H_2O)_2]Cl_3$. Yield 77 mg (58%). ^{1}H NMR (500 MHz, D_2O, 298 K): 8.09, 7.56, 4.56, 4.53, 4.45, 4.41, 3.81, 2.48, 1.83, 1.21, 1.16. Calcd (anal.) for $YC_{26}H_{48}N_6O_5Cl_3$: C, 43.65 (43.37); H, 6.38 (6.72); N, 11.68 (11.67).

RESULTS AND DISCUSSION

X-ray Crystal Structures. The structures of $[TmL^{RI}(H_2O)_2](NO_3)_3\cdot H_2O$ and $[LuL^{RI}(H_2O)_2](NO_3)_3\cdot H_2O$ (Supporting Information, Figure S1) are isomorphous to the previously reported Yb(III) derivative.[1] These complexes contain $[LnL^{RI}(H_2O)_2]^{3+}$ complex cations (Figure 2) with 8-coordinate Ln(III) ion coordinated by the six nitrogen atoms of the macrocycle L and two axial water molecules situated at the same side of the macrocycle. The asymmetric units of the isomorphous $[HoL^{RI}(NO_3)(H_2O)](NO_3)_2\cdot 0.4H_2O$ and $[ErL^{RI}(NO_3)(H_2O)](NO_3)_2\cdot 0.3H_2O$ crystals (Supporting Information, Figure S2) contain complex cation $[LnL^{RI}(H_2O)(NO_3)]^{2+}$ (Figure 2), two uncoordinated nitrate anions as well as partially occupied water molecule (see the Supporting Information for the description of disorder). In these complexes the Ln(III) ions adopt irregular 9-coordinate geometry and are coordinated by the six nitrogen atoms of the macrocycle L in addition to water molecule and nitrate anion positioned at the same side of the macrocycle. The differences in coordination number and axial ligation between the above two series of nitrate complexes Ho−Er and Tm−Lu reflect decreasing radii ions along the lanthanide series (Supporting Information, Table S1).

The asymmetric unit of the $[YL^{RI}Cl(H_2O)]Cl_2\cdot MeOH\cdot 2H_2O$ complex (Supporting Information, Figure S3) contains complex cation $[YL^{RI}Cl(H_2O)]^{2+}$ (Figure 3), two chloride anions, two water molecules, and a methanol molecule. The 8-coordinate Y(III) ion is coordinated by the six nitrogen atoms of the macrocycle L as well as axial water molecule and axial chloride positioned at the same side of the macrocycle. A similar complex cation (Figure 3) is observed in the crystal structure of $[YbL^{RI}Cl(H_2O)]Cl_2\cdot CH_3CN$ (Supporting Information, Figure S4), although the Y(III) and Yb(III) complexes are not isomorphous.

The asymmetric unit of $[SmL^{RII}(NO_3)(H_2O)_2](NO_3)_2$ contains two complex cations $[SmL^{RII}(NO_3)(H_2O)_2]^{2+}$ and four nitrate anions. This complex is isostructural with the previously reported Eu(III) and Pr(III) derivatives obtained by a different synthetic procedure.[1] The two independent complex cations are very similar. The 10-coordinate Sm(III) ions are coordinated by six nitrogen atoms of the macrocycle L, a bidentate nitrate anion located at one side of the macrocycle, and two water molecules located at the opposite side (Figure 4). The asymmetric unit of $[TbL^{RII}(NO_3)(H_2O)](NO_3)_2\cdot 0.3H_2O$ contains complex cation $[TbL^{RII}(NO_3)(H_2O)]^{2+}$, two nitrate anions, and a partially occupied water molecule. Similarly as in the case of the Sm(III) complex, an axial water molecule and nitrate anion are positioned at opposite faces of the macrocycle (Figure 4). The lower coordination number of the Tb(III) complex in comparison with the Sm(III) complex reflects the contraction of the lanthanide series.

In the above Ho(III), Er(III), Tm(III), and Lu(III) nitrate derivatives crystallized from water solutions and in the Y(III) and Yb(III) chloride derivatives crystallized from organic solvents the macrocyclic ligand adopts very similar conformation. In contrast, crystals of $[SmL^{RII}(NO_3)(H_2O)_2](NO_3)_2$ and $[TbL^{RII}(NO_3)(H_2O)](NO_3)_2\cdot 0.3H_2O$ complexes grown from organic solvents reveal a different conformation of the macrocycle (Figure 4, Supporting Information, Figures S5, S6). In the above Ho(III)−Yb(III) series of complexes of the macrocycle

dx.doi.org/10.1021/ic401437r | Inorg. Chem. 2013, 52, 12450−12460

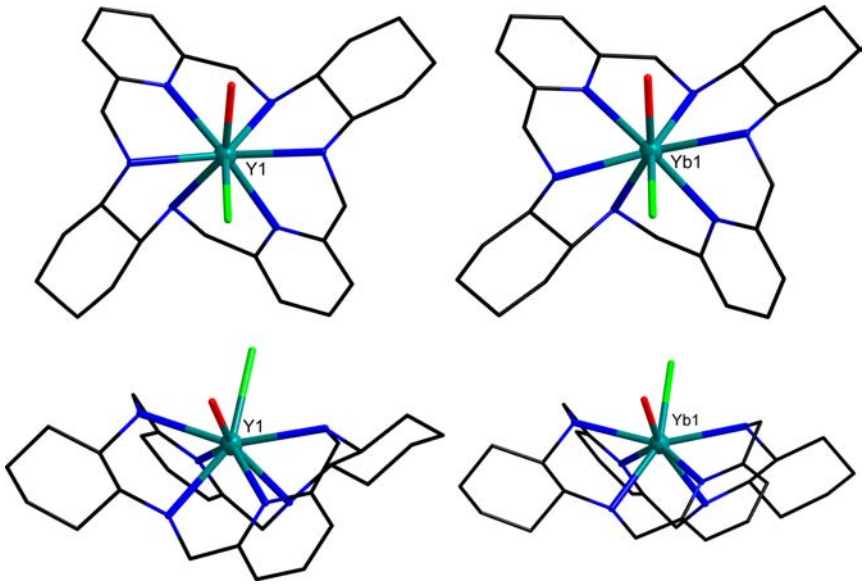

Figure 3. Structures of the $[YL^{RI}Cl(H_2O)]^{2+}$ (left) and $[YbL^{RI}Cl(H_2O)]^{2+}$ (right) complex cations.

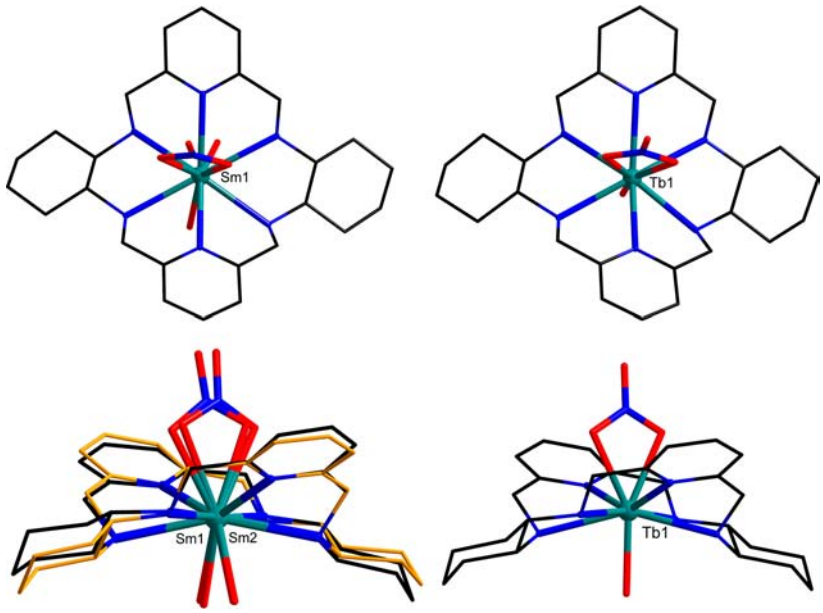

Figure 4. Structures of complex cations: $[SmL^{RII}(NO_3)(H_2O)_2]^{2+}$ (one of the two independent ions; left) and $[TbL^{RII}(NO_3)(H_2O)]^{2+}$ (right). The comparison of the geometry of the two independent $[SmL^{RII}(NO_3)(H_2O)_2]^{2+}$ ions is also shown (lower left).

L^R derived from *trans*-(1*R*,2*R*)-diaminocyclohexane, the chirality at the carbon atoms imposes also a specific configuration at the coordinated amine nitrogen atoms which results in formation of the L^{RI} diastereomer. In this diastereomer denoted as form I, the NH protons point alternately above and below the macrocycle plane. This conformation corresponds to the *RRRR* configuration[17] at the amine nitrogen atoms of the respective form of the free ligand L (Figure 1). In the Sm(III) and Tb(III) complexes a different diastereomer of L is present, denoted as form II. In this form all the amine protons NH of L^R point to one side of the macrocycle, corresponding to the *RSRS* configuration at the nitrogen atoms (Figure 1).

The two forms of complexes differ not only in the orientation of NH protons. In all complexes of diastereomer I the axial ligands are located at one side of the macrocycle, while in the complexes of diastereomer II they are positioned at both sides of the macrocycle (Figures 4, 5). In form I the ligand adopts a rather compact form as a result of wrapping around the metal ion as well as substantial bending of the macrocycle. This combination of twist and fold of the macrocycle makes only one side of the system available for the coordination of additional axial ligands. The conformation of the form II is dominated by the bending of the macrocycle. This bending is reflected by the angle determined by the two pyridine nitrogen atoms and the central metal ion, equal to 139.9(2)°, 139.5(2)° for two crystallographically independent cations in the Sm(III) complex, and equal to 145.69(11)° for the complex cation in the Tb(III) compound. Overall conformation of form II is more open in comparison with that of form I, so there is less steric hindrance for the coordination of ligands at *both* sides of the macrocycle.

dx.doi.org/10.1021/ic401437r | *Inorg. Chem.* 2013, 52, 12450−12460

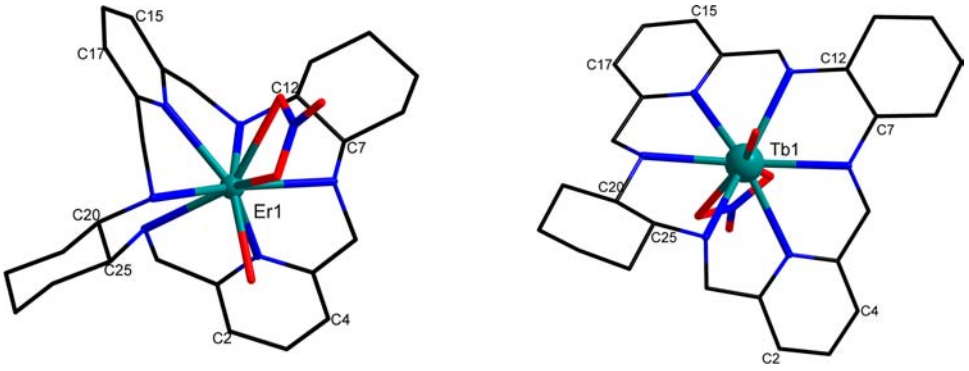

Figure 5. Comparison of the conformations of diastereomers I and II. The complex cation $[ErL^{RI}(NO_3)(H_2O)]^{2+}$ (left) contains diastereomeric form I and the complex cation $[TbL^{RII}(NO_3)(H_2O)]^{2+}$ (right) contains diastereomeric form II of macrocycle L.

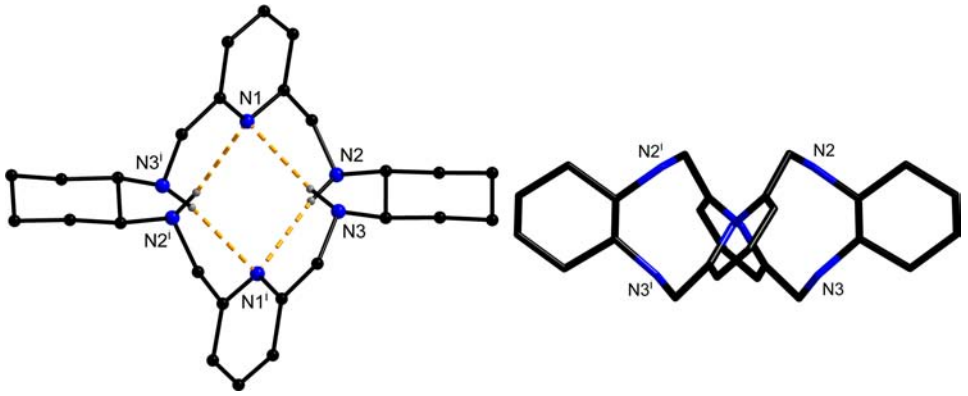

Figure 6. Top and side views of the free macrocycle L^R. Symmetry code (i): $-x+1, y, -z+1$.

Another difference between diastereomers I and II is the different mutual orientation of the cyclohexane fragments as well as the different mutual orientation of the pyridyl rings. The orientation of the cyclohexane rings is reflected by the pseudotorsion angle C7−C12−C20−C25 (Figure 5), which ranges from −64.1(3)° to −51.95(11)° for the complexes with diastereomer I (extreme values for $[HoL^{RI}(NO_3)(H_2O)]^{2+}$ and $[YL^{RI}Cl(H_2O)]^{2+}$, respectively) and ranges from 70.7(4)° to 79.5(5)° for the complexes with diastereomer II (extreme values for two crystallographically independent $[SmL^{RII}(NO_3)(H_2O)_2]^{2+}$ cations). The mutual orientation of pyridine rings is reflected by the pseudotorsion angle C2−C4−C15−C17, which is in the range from 83.23(7)° to 91.37(10)° for the complexes with diastereomer I (extreme values for $[YL^{RI}Cl(H_2O)]^{2+}$ and $[YbL^{RI}Cl(H_2O)]^{2+}$ cations, respectively) and in the range from −13.2(3)° to −10.0(3)° for the complexes with diastereomer II (extreme values for two crystallographically independent $[SmL^{RII}(NO_3)(H_2O)_2]^{2+}$ cations). The opposite signs of the above torsion angles for the forms I and II correspond to the opposite sense of the helical twist.

The helical twist of the macrocycle L is observed not only in its complexes but also in its free form obtained from chloroform solution. The X-ray crystal structure of the L^R enantiomer of the macrocycle shows a highly twisted conformation, accompanied by some additional bending (Figure 6). The molecule lies in a special position, on a 2-fold axis passing through the center of the macrocycle (but through none of its atoms). The mutual orientation of cyclohexane rings is reflected by the pseudotorsion angle C7−C12−$C7^i$−$C12^i$ equal to −86.1(4)°, and the mutual orientation of the pyridine rings is reflected by the pseudotorsion angle C2−C4−$C2^i$−$C4^i$ equal to 98.9(3)° (symmetry code is given in Figure 6). These values correspond to the conformation of diastereomeric form I. On the other hand, for the free macrocycle in solution the positions of the amine hydrogen atoms may vary, and the geometry at the nitrogen atoms is not necessarily fixed because of dynamic processes. The conformation of the free L is quite similar to that found in the diastereomeric form I Ln(III) complexes and even more to that found in the Cd(II) and Zn(II) complexes[2] of L. This similarity indicates that this macrocycle is preorganized to form helical complexes of type I and need not to wrap around the metal ions from a putative more flat conformation. On the other hand, the additional bending of Ln(III) complexes of type I, as well as formation of Ln(III) complexes of type II, reflect less than perfect fit between the cavity size of the free macrocycle and the size of the Ln(III) ions as well as the steric effects of axial ligands.

Synthesis and Spectroscopic Characterization of the Complexes. The $[LnL^{RI}(H_2O)_2](NO_3)_3$ complexes can be easily obtained in water solvent using the L^R enantiomer of the macrocycle and nitrate salts of the heavier lanthanides Tm(III), Yb(III), and Lu(III). In the case of Ho(III) and Er(III) the $[LnL^{RI}(NO_3)(H_2O)](NO_3)_2$ complexes are obtained under analogous conditions. Similarly, chloride derivatives of the type $[LnL^{RI}(H_2O)_2]Cl_3$ can be obtained in water using chloride salts of the heavier lanthanides Tm(III), Yb(III), and Lu(III) or Y(III) as substrates. The CD spectra and X-ray crystal structures of the above complexes indicate that the diastereomeric form I corresponding to the *RI* chirality is preferred for complexes synthesized in water. This form seems to be more

dx.doi.org/10.1021/ic401437r | *Inorg. Chem.* 2013, 52, 12450−12460

compatible with smaller (heavier) lanthanide(III) ions. In the case of nitrate salts of lighter lanthanides, such as Sm(III) or Tb(III), insoluble products were obtained, which could be recrystallized from organic solvents to give $[SmL^{RII}(NO_3)(H_2O)_2](NO_3)_2$ and $[TbL^{RII}(NO_3)(H_2O)](NO_3)_2{\cdot}0.3H_2O$ complexes containing diastereomeric form II of macrocycle L. This different form of the macrocycle gives rise to a different type of solution CD spectra (Supporting Information, Figure S7). The complexes of form I and form II exhibit different CD spectra also for the solid samples measured as KCl pellets, in particular in the region around 200 nm (Supporting Information, Figure S8).

In general, smaller Ln(III) ions seem to prefer form I of the ligand, while the larger Ln(III) ions seem to prefer form II. However, the type of the diastereomer of the ligand is not solely determined by the type of the Ln(III) ion, as we have observed both forms of the macrocycle L with the same ion, Yb(III).[1] Equally or more important is the solvent used for synthesis; complexes of form I are preferred in the case of water, while complexes of form II are preferred in the case of organic solvents.

The ^{1}H NMR spectra of the obtained lanthanide(III) complexes indicate C_2 symmetry corresponding to the presence of 19 signals of equal intensity. It should be also noted that the exchange of NH protons for deuterium in D_2O solutions is very slow (the NH signals do not completely vanish even after 2 weeks, Supporting Information, Figure S9). This behavior is characteristic for strongly coordinated secondary amine nitrogen atoms that slowly undergo inversion or exchange for deuterium.[5,8] In the case of paramagnetic Ln(III) complexes the signals span a wide range of chemical shifts (Figure 7),

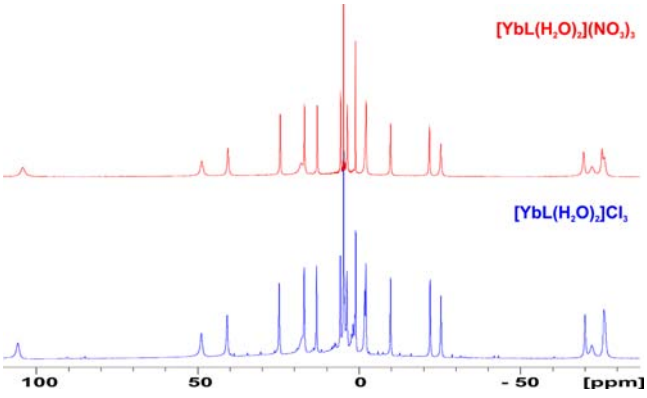

Figure 7. Comparison of the ^{1}H NMR spectra (300 MHz, 298 K) of the D_2O solutions (pH = 6.5) of complexes $[YbL^{RI}(H_2O)_2](NO_3)_3$ (top) and $[YbL^{RI}(H_2O)_2]Cl_3$ (bottom).

while some of the signals are not observed because of paramagnetic broadening, particularly for the Tb(III), Ho(III), and Er(III) derivatives. The C_2 symmetry is also in accord with the 2D NMR spectra measured for the D_2O solution of the diamagnetic $[LuL^{RI}(H_2O)_2](NO_3)_3$ complex (Figure 8, Supporting Information, Figures S10−S12). The signals of this complex can be assigned starting from the HMQC spectrum (Supporting Information, Figure S11) identifying the two amine proton signals e1 and e2 (see Figure 8 for the labeling scheme). These are in turn COSY correlated (Supporting Information, Figure S10) to the two analogous signals of axial methylene protons d1, d2, as well as to the cyclohexane signals f1 and f2. The combined analysis of COSY and HMQC spectrum allows full ^{13}C and ^{1}H NMR spectral assignment, even though the pair of signals b1 and b2, c1 and d2, c2 and d1, i1 and i2 as well as j1 and j2 are overlapped. This signal assignment is confirmed by the NOESY spectrum (Figure 8). Apart from the expected negative NOE-type cross-peaks, additional positive exchange-type cross-peaks are observed in the NOESY (Figure 8) and ROESY (Supporting Information, Figure S12) spectra. These exchange-type correlations between signals of c1 and c2, d1 and d2, f1 and f2, g1 and g2 as well as h1 and h2 indicate a chemical exchange process that interconverts the positions denoted with 1 and those denoted with 2 (Figure 8, Supporting Information, Figure S13). This process corresponds to the dissociation of axial water molecules at one side of the macrocycle followed by coordination of these molecules at the opposite side, accompanied by the adjustment of the macrocycle conformation (Supporting Information, Figures S13, S14). In the case of water solution of the $[YL^{RI}(H_2O)_2]Cl_3$ complex, the analogous exchange of water molecules at the two sides of the macrocycle is fast enough to average the corresponding pairs of signals and the observed ^{1}H, and ^{13}C NMR spectra correspond to effective D_2 symmetry (Supporting Information, Figures S15−S18). The averaging of the signals and the higher effective symmetry for the Y(III) complex is not related to enantiomerization of the complex (Supporting Information,. Figure S14), as it was observed for the Ln(III) complex with the other macrocyclic ligand.[18] The slower dynamic process for the Lu(III) complex in comparison with that of the Y(III) complex reflects its smaller size, higher charge density, and stronger bonds. A similar influence of rare earth ion size on the rigidity of complexes and the number of ligand NMR signals has been observed previously for the series of lanthanide(III) complexes with other ligands.[19]

In the case of Tm(III), Yb(III), and Lu(III) derivatives practically identical CD (Supporting Information, Figure S19) and ^{1}H NMR spectra (Figure 7, Supporting Information, Figure S20) are observed for the pairs of complexes $[LnL^{RI}(H_2O)_2](NO_3)_3/[LnL^{RI}(H_2O)_2]Cl_3$. As expected, the enantiomeric complexes, for example, $[YbL^{RI}(H_2O)_2](NO_3)_3$ and $[YbL^{SI}(H_2O)_2](NO_3)_3$, give mirror-like CD spectra (Supporting Information, Figure S21). Because the NMR spectra of paramagnetic macrocyclic Ln(III) complexes are extremely sensitive to the type of axial ligand, the identical spectra for the chloride and nitrate derivatives indicate that neither nitrate nor chloride anions are coordinated to the Ln(III) in water solutions. In these solutions complex cations $[LnL^{RI}(H_2O)_2]^{3+}$ containing water molecule as axial ligands are present. It is likely that the same type of cation is present in the water solutions of the Y(III) derivative instead of the $[YL^{RI}Cl(H_2O)]^{2+}$ complex cation observed in the crystal structure. Similarly the bulk chloride Yb(III) and Y(III) derivatives synthesized from water solutions more likely correspond to the formula $[LnL^{RI}(H_2O)_2]Cl_3$ rather than the formula $[LnL^{RI}Cl(H_2O)]Cl_2$ corresponding to the crystal structures of complexes crystallized from organic solvent.

In contrast to the situation observed for water solutions, different CD (Supporting Information, Figures S22, S23) and ^{1}H NMR spectra (Supporting Information, Figures S24, S25) are observed for the pairs of complexes $[LnL^{RI}(H_2O)_2](NO_3)_3/[LnL^{RI}(H_2O)_2]Cl_3$ freshly dissolved in methanol or acetonitrile. This difference must reflect the coordination of counter-anions as axial ligands in the complex forms present in organic solutions.

dx.doi.org/10.1021/ic401437r | Inorg. Chem. 2013, 52, 12450−12460

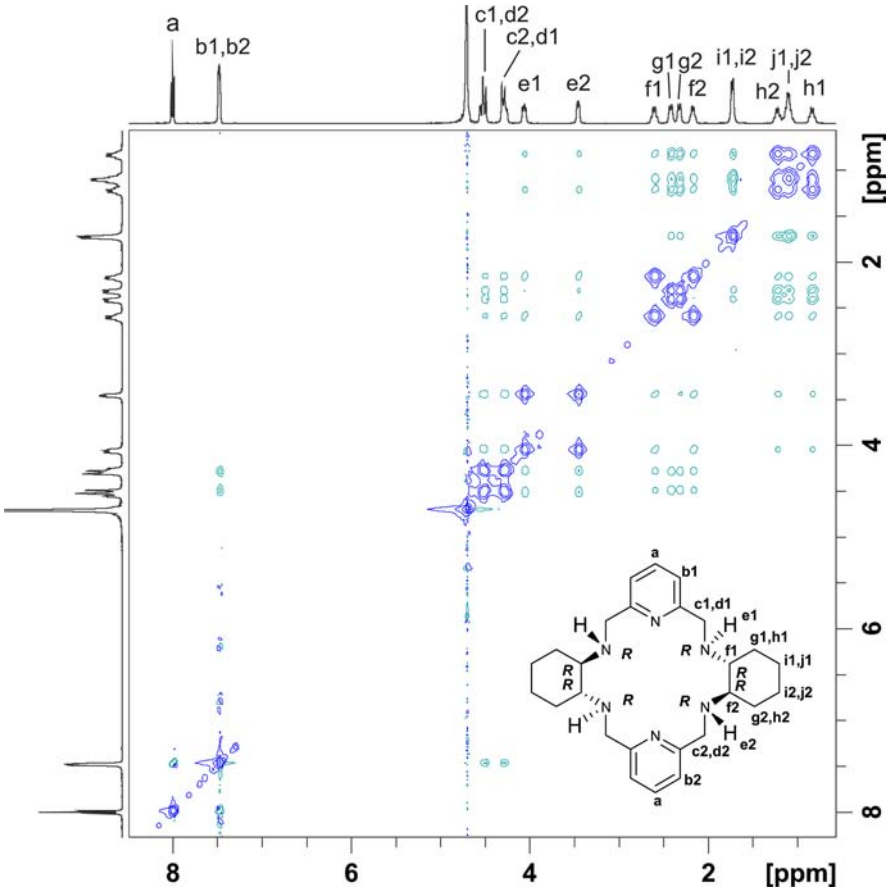

Figure 8. NOESY spectrum of the D_2O solution of the $[LuL^{RI}(H_2O)_2](NO_3)_3$ complex (pH = 6.5). Green lines correspond to NOE-type correlations and blue lines to exchange-type correlations.

Chirality Inversion. The CD spectra of water solutions of the $[LnL^{RI}(H_2O)_2](NO_3)_3$ (Ln = Tm, Lu) and $[LnL^{RI}(NO_3)(H_2O)](NO_3)_2$ (Ln = Ho, Er) complexes do not change over time. In contrast the CD spectra of the same complexes in methanol or acetonitrile solutions gradually change. This change corresponds to the inversion of helicity of the complexes and transformation of the diastereomeric form I to the diastereomeric form II (Figure 9). We have documented previously similar process for the Yb(III) complexes, where both diastereomeric forms were synthesized and structurally characterized.[1] The conversion of form I to form II is also reflected in gradual change of ^1H NMR spectra, as the two types of complexes give rise to different signals (Figure 10, Supporting Information, Figure S24). It should be noted that the NMR spectra measured immediately after dissolution of the $[LnL^{RI}(H_2O)_2](NO_3)_3$ (Ln = Tm, Yb, Lu) complexes in CD_3OD or CD_3CN are markedly different from those recorded for D_2O solutions of these complexes. The lines are severely

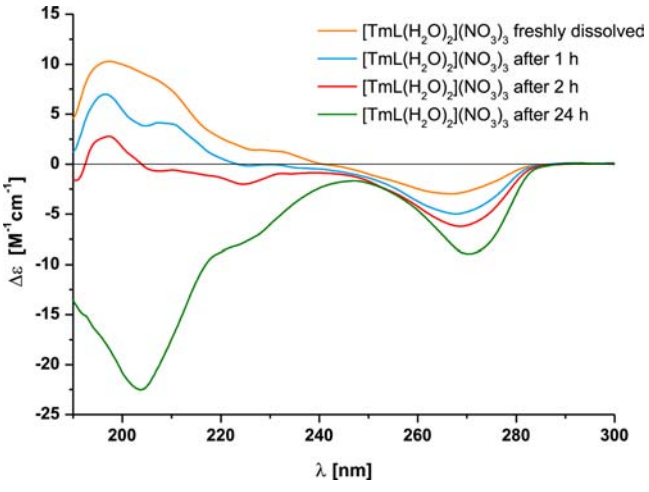

Figure 9. Time-dependent CD spectra of 0.25 mM acetonitrile solutions of the $[TmL^{RI}(H_2O)_2](NO_3)_3$ complex.

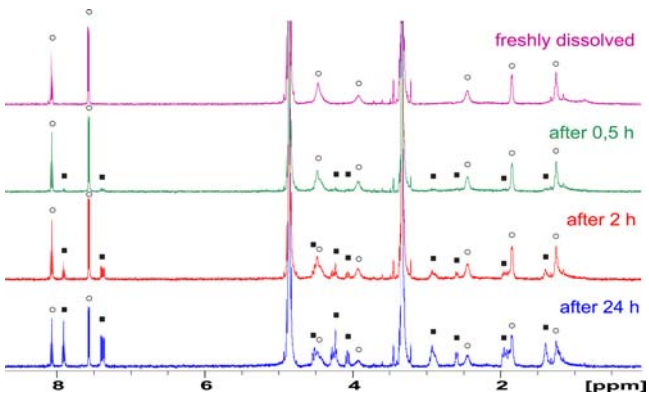

Figure 10. Time-dependent ^1H NMR spectra recorded for the CD_3OD solution of $[LuL^{RI}(H_2O)_2](NO_3)_3$. Open circles indicate signals of diastereomer I, squares indicate signals of diastereomer II.

dx.doi.org/10.1021/ic401437r | Inorg. Chem. 2013, 52, 12450−12460

broadened and correspond to decisively different chemical shifts. This difference has to arise from replacement of at least part of the axial water molecules by nitrate anions bound in axial positions. The additional line broadening indicates chemical exchange effects superimposed on paramagnetic relaxation. Although the exact nature of the complex form present at this stage is not known, most likely it corresponds to species with two axial nitrate ligands $[LnL^{RI}(NO_3)_2]^+$ in equilibrium with other forms such as $[LnL^{RI}(NO_3)(H_2O)]^{2+}$. The formation of cations $[LnL^{RI}(NO_3)_2]^+$ is practically immediate, as the ligand exchange in macrocyclic complexes of fluxional Ln(III) ions is a fast process. The subsequent spectral changes reflect much slower macrocycle rearrangement to diastereomeric form II in the $[LnL^{RII}(NO_3)_2]^+$ cation.

The comparison of the CD spectra measured over time for the series of Tm–Lu nitrate derivatives indicates decreasing extent of spectral changes (Figure 9 and Supporting Information, Figure S22), suggesting that for the $[LuL^{RI}(H_2O)_2](NO_3)_3$ the conversion is incomplete. This conclusion is supported by the comparison of spectral changes in the ^{1}H NMR spectra recorded over time for this series of nitrate complexes in organic solvents. While the conversion of complex form I to complex form II is practically complete for the Tm(III) complex and almost complete for the Yb(III) complexes (Supporting Information, Figure S24), the equilibrium corresponding roughly to equal concentrations of form I and II is reached for the Lu(III) derivative (Figure 10). These differences reflect the preference of the smallest Lu(III) ion for the more compact, twisted form I. This preference is not fully reversed by the application of organic solvent.

In contrast to the behavior of nitrate derivatives, the CD and ^{1}H NMR spectra of chloride derivatives $[LnL^{RI}(H_2O)_2]Cl_3$ (Ln = Tm, Yb, Lu) do not change over time both for water solutions and for the methanol or acetonitrile solutions (Supporting Information, Figure S23). This difference shows that the conversion of diastereomeric form I to form II is anion dependent. Most likely it reflects the tendency of nitrate anion to axial coordination in a bidentate mode. In contrast to water solvent used for the synthesis, the organic solvents used for the monitoring of spectral changes favor less ionic complex forms, for example, $[LnL^{RII}(NO_3)_2]^+$ cation in comparison with the original $[LnL^{RI}(H_2O)_2]^{3+}$ cation. The observed chirality inversion is likely related to sterical preferences of the two forms. In the more compact form I less space is available for the coordination of two axial bidentate ligands at the same face of the macrocycle. In a more "flat" form II the axial ligands can be bound at both faces of the macrocycle, thus enabling formation of 10-coordinate complexes with two bidentate nitrate anions. This mechanism explains the reason why the chloride derivatives do not undergo diastereomeric conversion in organic solvents: the monodentate chloride axial ligand is less sterically demanding in comparison with the bidentate nitrate ligand. Additionally, the chloride anion has a lower tendency to coordinate to the hard Ln(III) ions and competes less strongly with water molecules for axial coordination sites. Indeed the comparison of the NMR spectra of the freshly prepared solutions of the paramagnetic complexes $[TmL^{RI}(H_2O)_2]Cl_3$ and $[YbL^{RI}(H_2O)_2]Cl_3$ in CD_3OD with those in D_2O reveals quite similar spectra. This similarity most likely points to a limited replacement of axial water molecules and formation of species such as $[LnL^{RI}Cl(H_2O)]^{2+}$ and $[LnL^{RI}Cl_2]^+$, which are in a (fast on the NMR time scale) equilibrium with the intact dominant cation $[LnL^{RI}(H_2O)_2]^{3+}$.

Since axial ligands can be easily exchanged in the macrocyclic Ln(III) complexes,[3b,20] the above mechanism should be verified by exchange of the chloride counteranion for the nitrate counteranion; this exchange should trigger the chirality inversion process. To test this hypothesis we have added sodium nitrate to solutions of $[LnL^{RI}(H_2O)_2]Cl_3$ (Ln = Tm, Yb, Lu) complexes in methanol and monitored the reaction by CD and ^{1}H NMR. The exchange of anion resulted in the immediate change of the CD spectrum, which then gradually changed again over time (Figure 11). The change of the

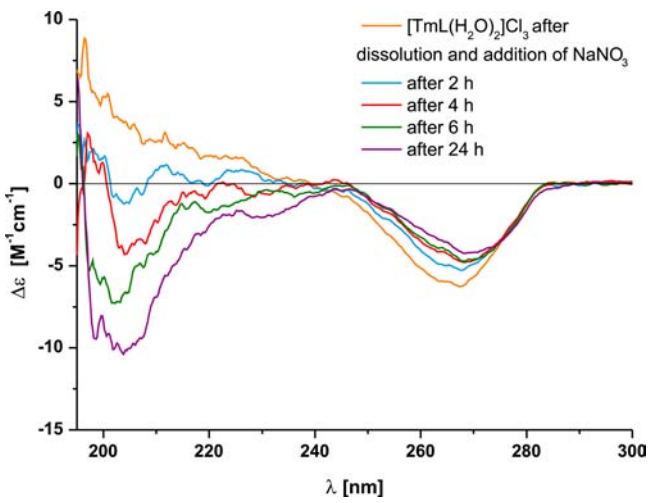

Figure 11. Time-dependent CD spectra of 0.125 mM methanol solution of $[TmL^{RI}(H_2O)_2]Cl_3$ complex measured after addition of $NaNO_3$ (0.75 mM).

spectrum immediately after addition of nitrate anions reflects axial ligand exchange, since it is a fast process for Ln(III) macrocyclic complexes.[3b,20] Similar behavior was also reflected by the ^{1}H NMR spectra. For instance the spectrum measured directly after addition of 6 equiv of $NaNO_3$ to the solution of $[YbL^{RI}(H_2O)_2]Cl_3$ in CD_3OD indicates a dynamic mixture of species such as $[YbL^{RI}Cl(NO_3)]^+$, $YbL^{RI}(NO_3)(H_2O)]^{2+}$, or $[YbL^{RI}(NO_3)_2]^+$. With time a new set of signals gradually appear, which dominate the spectrum measured after 24 h (Supporting Information, Figure S26). The spectral pattern of the final species is similar, but not identical to that of the final species obtained for the nitrate derivative, that is to the $[YbL^{RII}(NO_3)_2]^+$ complex cation (Supporting Information, Figure S27). Nevertheless the final product is a $[YbL^{RII}(NO_3)_2]^+$ cation in equilibrium (fast on the NMR time scale) with species such as $[YbL^{RII}(NO_3)Cl]^+$ or $[YbL^{RII}Cl_2]^+$. The replacement of chloride for nitrate is simply not complete and both anions compete for the Ln(III) ion complexed by diastereomeric form II of the macrocycle. This can be proved by gradual addition of chloride anions to the solution of the final $[YbL^{RII}(NO_3)_2]^+$ complex resulting from the conversion of $[YbL^{RI}(H_2O)_2](NO_3)_3$ in CD_3OD. The ^{1}H NMR spectrum recorded for such a titration experiment is practically identical to the final spectrum recorded for the reaction of chloride complex with $NaNO_3$ (Supporting Information, Figure S28). In summary, the nitrate anion can replace the chloride anion in the $[YbL^{RI}(H_2O)_2]Cl_3$ complexes and trigger chirality inversion, although this process is partly obscured by mixed species of the type $[YbL^{RI}(NO_3)Cl]^+$ and $[YbL^{RII}(NO_3)Cl]^+$. A similar situation was observed for the addition of $NaNO_3$ to the chloride complexes of Tm(III) and

dx.doi.org/10.1021/ic401437r | Inorg. Chem. 2013, 52, 12450–12460

Lu(III) (Supporting Information, Figure S26). In the case of Lu(III) derivative only partial conversion of form I to form II is observed, similarly to what was observed for the nitrate complex itself.

CONCLUSIONS

The crystal structures of the lanthanide(III) complexes with chiral macrocycle L indicate that this ligand can exist in diastereomeric forms I and II. Form I is more compact as a result of considerable twist and fold of the macrocycle, and this form imposes coordination of axial ligands at the same face of the macrocycle. The nitrate complexes $[LnL^{RI}(H_2O)_2](NO_3)_3$ (Ln = Ho−Lu) of the diastereomeric form I of the ligand slowly convert to complexes of the diastereomeric form II after dissolution in organic solvents. This process of chirality inversion in organic solvent is not observed for analogous chloride derivatives. It can be triggered, however, by addition of external nitrate anions to $[LnL^{RI}(H_2O)_2]Cl_3$ (Ln = Tm−Lu) complexes. This addition results in initial fast anion exchange, followed by a slow chirality inversion process. The simplified chirality inversion scheme for the Tm(III), Yb(III), and Lu(III) complexes is presented below.

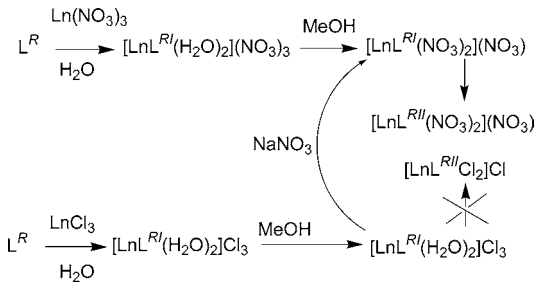

ASSOCIATED CONTENT

Supporting Information

Details of the structure refinment, Figures S1−S28 (^{1}H NMR and CD spectra, views of molecular structures) as well as X-ray crystallographic information in CIF format. This material is available free of charge via the Internet at http://pubs.acs.org.

AUTHOR INFORMATION

Corresponding Author

*E-mail: jerzy.lisowski@chem.uni.wroc.pl. Fax: 48 71 3282348. Phone: 48 71 3757252.

Notes

The authors declare no competing financial interest.

ACKNOWLEDGMENTS

This work was supported by Grant 2260/M/WCH/12.

REFERENCES

(1) Gregoliński, J.; Ślepokura, K.; Lisowski, J. *Inorg. Chem.* **2007**, *46*, 7923−7934.

(2) Bligh, S. W. A.; Choi, N.; Evagorou, E. G.; Li, W.-S.; McPartlin, M. *Chem. Commun.* **1994**, 2399−2400.

(3) (a) Lisowski, J. *Inorg. Chem.* **2011**, *50*, 5567−5576. (b) Lisowski, J.; Ripoli, S.; Di Bari, L. *Inorg. Chem.* **2004**, *43*, 1388−1394. (c) Lisowski, J.; Mazurek, J. *Polyhedron* **2002**, *21*, 811−816. (d) Lisowski, J.; Starynowicz, P. *Polyhedron* **2000**, *19*, 465−469. (e) Tsubomura, T.; Yasaku, K.; Sato, T.; Morita, M. *Inorg. Chem.* **1992**, *31*, 447−450.

(4) (a) Krężel, A.; Lisowski, J. *J. Inorg. Biochem.* **2012**, *107*, 1−5. (b) Zhao, C.; Ren, J.; Gregolinski, J.; Lisowski, J.; Qu, X. *Nucleic Acids Res.* **2012**, *40*, 8186. (c) Bligh, S. W. A.; Choi, N.; Evagorou, E. G.; McPartlin, M.; White, K. N. *J. Chem. Soc., Dalton Trans.* **2001**, 3169−3172.

(5) (a) Gregoliński, J.; Starynowicz, P.; Hua, K. T.; Lunkley, J. L.; Muller, G.; Lisowski, J. *J. Am. Chem. Soc.* **2008**, *130*, 17761−17773. (b) Gregoliński, J.; Lis, T.; Cyganik, M.; Lisowski, J. *Inorg. Chem.* **2008**, *47*, 11527−11534. (c) Gregoliński, J.; Lisowski, J. *Angew. Chem., Int. Ed.* **2006**, *45*, 6122−6126.

(6) Gonzalez-Alvarez, A.; Alfonso, I.; Cano, J.; Diaz, P.; Gotor, V.; Gotor-Fernandez, V.; Garcia-Espana, E.; Garcia-Granda, S.; Jimenez, H. R.; Lloret, G. *Angew. Chem., Int. Ed.* **2009**, *48*, 6055−6058.

(7) See for example: (a) El Ghachtouli, S.; Cadiou, C.; Déchamps-Olivier, I.; Chuburu, F.; Aplincourt, M.; Roisnel, T. *Eur. J. Inorg. Chem.* **2006**, 3472−3481. (b) Bucher, C.; Moutet, J. C.; Pécaut, J.; Royal, G.; Saint-Aman, E.; Thomas, F.; Torelli, S.; Ungureanu, M. *Inorg. Chem.* **2003**, *42*, 2242−2252. (c) Bucher, C.; Moutet, J.-C.; Pécaut, J.; Royal, G.; Saint-Aman, E.; Thomas, F. *Inorg. Chem.* **2004**, *43*, 3777−3779. (d) Bosnich, B.; Tobe, M. L.; Webb, G. A. *Inorg. Chem.* **1965**, *4*, 1109−1112. (e) Creutz, C.; Chou, M. H.; Fujita, E.; Szalda, D. J. *Coord. Chem. Rev.* **2005**, *249*, 375−390. (f) Liang, X.; Sadler, P. J. *Chem. Soc. Rev.* **2004**, *33*, 246−266. (g) Madej, E.; Monsted, O.; Kita, P. *J. Chem. Soc., Dalton Trans.* **2002**, 2361−2365. (h) Haines, R. I.; Hutchings, D. R.; McCormack, T. M. *J. Inorg. Biochem.* **2001**, *85*, 1−7. (i) Curtis, N. F. *Inorg. Chim. Acta* **2001**, *317*, 27−32. (j) Slocik, J. M.; Ward, M. S.; Shepherd, R. E. *Inorg. Chim. Acta* **2001**, *317*, 290−303.

(8) (a) Liang, X.; Weishäupl, M.; Parkinson, J. A.; Parsons, S.; McGregor, P. A.; Sadler, P. J. *Chem.—Eur. J.* **2003**, *9*, 4709−4717. (b) Liang, X.; Parkinson, J. A.; Weishäupl, M.; Gould, R. O.; Paisey, S. J.; Park, H.; Hunter, T. M.; Blindauer, C. A.; Parsons, S.; Sadler, P. J. *J. Am. Chem. Soc.* **2002**, *124*, 9105−9112. (c) Buckingham, D. A.; Clark, C. R.; Rogers, A. J. *J. Am. Chem. Soc.* **1997**, *119*, 4050−4058.

(9) (a) Miyake, H.; Tsukube, H. *Chem. Soc. Rev.* **2012**, *41*, 6977−6991. (b) Dai, Z.; Lee, J.; Zhang, W. *Molecules* **2012**, *17*, 1247−1277. (c) Canary, J. W.; Mortezaei, S.; Liang, J. *Coord. Chem. Rev.* **2010**, *254*, 2249−2266. (d) Crassous, J. *Chem. Soc. Rev.* **2009**, *38*, 830−845. (e) Hembury, G. A.; Borovkov, V. V.; Inoue, Y. *Chem. Rev.* **2008**, *108*, 1−73. (f) Belmont, P.; Constant, J.-F.; Demeunynck, M. *Chem. Soc. Rev.* **2001**, *30*, 70−81.

(10) For selected examples of controlled helicity inversion in inorganic systems: (a) Miyake, H.; Ueda, M.; Murota, S.; Sugimoto, H.; Tsukube, H. *Chem. Commun.* **2012**, *48*, 372−3723. (b) Akine, S.; Hotate, S.; Nabeshima, T. *J. Am. Chem. Soc.* **2011**, *133*, 13868−13871. (c) Ballistreri, F. P.; Gentile, S.; Pappalardo, A.; Tomaselli, G. A.; Pradhan, S.; Di Bari, L. *Chem.—Eur. J.* **2011**, *17*, 322−328. (d) Martinez, A.; Guy, L.; Dutasta, J.-P. *J. Am. Chem. Soc.* **2010**, *132*, 16733−16734. (e) Haberhauer, G. *Angew. Chem., Int. Ed.* **2010**, *49*, 9286−9289. (f) Miyake, H.; Hikita, M.; Itazaki, M.; Nakazawa, H.; Sugimoto, H.; Tsukube, H. *Chem.—Eur. J.* **2008**, *14*, 5393−5396. (g) Miyake, H.; Kamon, H.; Miyahara, I.; Sugimoto, H.; Tsukube, H. *J. Am. Chem. Soc.* **2008**, *130*, 792−793. (h) Montgomery, C. P.; New, E. J.; Parker, D.; Peacock, R. D. *Chem. Commun.* **2008**, 4261−4263. (i) Zahn, S.; Das, D.; Canary, J. W. *Inorg. Chem.* **2006**, *45*, 6056−6063. (j) Hutin, M.; Nitschke, J. *Chem. Commun.* **2006**, 1724−1726. (k) Miyake, H.; Sugimoto, H.; Tamiaki, H.; Tsukube, H. *Chem. Commun.* **2005**, 4291−4293. (l) Miyake, H.; Yoshida, K.; Sugimoto, H.; Tsukube, H. *J. Am. Chem. Soc.* **2004**, *126*, 6524−6525. (m) Zahn, S.; Canary, J. W. *Science* **2000**, *288*, 1404−1407. (n) Biscarini, P.; Kuroda, R. *Inorg. Chim. Acta* **1988**, *154*, 209−214.

(11) For selected examples of controlled helicity inversion in organic systems see: (a) Chen, C.-T.; Chen, C.-H.; Ong, T.-G. *J. Am. Chem. Soc.* **2013**, *135*, 5294−5297. (b) Pijper, D.; Jongejan, M. G. M.; Meetsma, A.; Feringa, B. L. *J. Am. Chem. Soc.* **2008**, *130*, 4541−4552. (c) Johnson, R. S.; Yamazaki, T.; Kovalenko, A.; Fenniri, H. *J. Am. Chem. Soc.* **2007**, *129*, 5735−5743. (d) Vicario, J.; Katsonis, N.; Serrano Ramon, B.; Bastiaansen, C. W. M.; Broer, D. J.; Feringa, B. L. *Nature* **2006**, *440*, 163. (e) Okoshi, K.; Sakurai, S.-i.; Ohsawa, S.; Kumaki, J.; Yashima, E. *Angew. Chem., Int. Ed.* **2006**, *45*, 8173−8176.

(f) Ajayaghosh, A.; Varghese, R.; George, S. J.; Vijayakumar, C. *Angew. Chem., Int. Ed.* **2006**, *45*, 1141−1144. (g) Sakurai, S.-i.; Okoshi, K.; Kumaki, J.; Yashima, E. *J. Am. Chem. Soc.* **2006**, *128*, 5650−5651. (h) Maeda, K.; Mochizuki, H.; Watanabe, M.; Yashima, E. *J. Am. Chem. Soc.* **2006**, *128*, 7639−7650. (i) Tang, H.-Z.; Novak, B. M.; He, J.; Polavarapu, P. L. *Angew. Chem., Int. Ed.* **2005**, *44*, 7298−7301. (j) Lohr, A.; Lysetska, M.; Würthner, F. *Angew. Chem., Int. Ed.* **2005**, *44*, 5071−5074. (k) Tang, H.-Z.; Boyle, P. D.; Novak, B. M. *J. Am. Chem. Soc.* **2005**, *127*, 2136−2142. (l) Tang, K.; Green, M. M.; Cheon, K. S.; Selinger, J. V.; Garetz, B. A. *J. Am. Chem. Soc.* **2003**, *125*, 7313−7323.

(12) (a) Suk, J.-M.; Naidu, V. R.; Liu, X.; Lah, M. S.; Jeong, K.-S. *J. Am. Chem. Soc.* **2011**, *133*, 13938−13841. (b) Meudtner, R. M.; Hecht, S. *Angew. Chem., Int. Ed.* **2008**, *47*, 4926−4930.

(13) Krężel, A.; Bal, W. *J. Inorg. Biochem.* **2004**, *98*, 161−166.

(14) *Crysalis CCD and Crysalis RED in Xcalibur PX, Xcalibur R or Kuma KM4CCD Software*; Oxford Diffraction Ltd.: Abingdon, England, 2009.

(15) Sheldrick, G. M. *Acta Crystallogr., Sect. A* **2008**, *64*, 112−122.

(16) Brandenburg, K. *DIAMOND*, Version 3.0; Crystal Impact GbR: Bonn, Germany, 2005.

(17) We indicate the chirality at the nitrogen atoms for the corresponding free macrocycle (Figure 1). As a consequence of CIP rules the reverse descriptors correspond to metal complexes, i.e., the *RRRR* configuration at amine nitrogen atoms in a putative rigid form of the free macrocycle correspond to the *SSSS* configuration at the same atoms in the complexed form.

(18) Castro, G.; Bastida, R.; Macías, A.; Pèrez-Lourido, P.; Platas-Iglesias, C.; Valencia, L. *Inorg. Chem.* **2013**, *52*, 6062−6072.

(19) (a) Tei, L.; Baranyai, Z.; Cassino, C.; Fekete, M.; Kálmán, F. K.; Botta, M. *Dalton. Trans.* **2012**, *41*, 12797−12806. (b) Tei, L.; Baranyai, Z.; Brücher, E.; Cassino, C.; Demicheli, F.; Masciocchi, N.; Giovenzana, G. B.; Botta, M. *Inorg. Chem.* **2010**, *49*, 616−625. (c) Mato-Iglesias, M.; Rodríguez-Blas, T.; Platas-Iglesias, C.; Starck, M.; Kadjane, P.; Ziessel, R.; Charbonnière, L. *Inorg. Chem.* **2009**, *48*, 1507−1518. (d) Platas-Iglesias, C.; Mato-Iglesias, M.; Djanashvili, K.; Muller, R. N.; Vander Elst, L.; Peters, J. A.; de Blas, A.; Rodríguez-Blas, T. *Chem.—Eur. J.* **2004**, *10*, 3579−3590. (e) Platas, C.; Avecilla, F.; de Blas, A.; Geraldes, C. F. G. C.; Rodríguez-Blas, T.; Adams, H.; Mahía, J. *Inorg. Chem.* **1999**, *38*, 3190−3199. (f) Zucchi, G.; Scopelliti, R.; Pittet, P.-A.; Bünzli, J.-C. G.; Rogers, R. D. *J. Chem. Soc., Dalton Trans.* **1999**, 931−938.

(20) Lisowski, J.; Sessler, J. L.; Lynch, V.; Mody, T. D. *J. Am. Chem. Soc.* **1995**, *117*, 2273−2285.